# Separated Flow Predictions Using a Hybrid $k$-$L$/Backflow Model

Uriel C. Goldberg* and Sukumar R. Chakravarthy†
*Rockwell International Science Center, Thousand Oaks, California 91310*

**A new hybrid one-equation $k$-$L$/backflow model has been used to compute several turbulent flow problems involving detached flow regions. The model incorporates algebraic near-wall treatments for the kinetic energy of turbulence $k$, the length scale $L$, and the eddy viscosity $\mu_t$. The near-wall formulation depends on whether the flow is attached or detached. This approach obviates the need to use wall functions. Agreement between predictions and experimental data is generally very good throughout the Mach number range.**

## Introduction

RECENTLY, a hybrid Baldwin-Lomax/backflow model has been applied successfully to predict a variety of separated turbulent flows.[1-3] Since the model is an algebraic one, it was necessary to invoke an ad hoc method in order to produce a turbulence history effect of the detached flow region on the flow downstream of reattachment (if such a region exists). When a transport equation for the kinetic energy of turbulence is introduced, these history effects are automatically taken into account.

In the present paper, a one-equation $k$-$L$ turbulence model is described in some detail, and results are shown for several flow problems involving detached flow regions at transonic, supersonic, and hypersonic flow regimes.

## The $k$-$L$ Turbulence Model

The $k$-$L$ turbulence model combines a partial differential equation for the kinetic energy of turbulence ($k$) with an algebraic expression for the distribution of the length scale ($L$). Thus, the velocity scale distribution within the flowfield, $\sqrt{k}$, is determined from a well-established and reliable equation (the $k$ equation) while retaining the degrees of freedom afforded through the algebraic approach to the determination of the length scale. For example, length scale distributions can be tailormade for wall/wake shear layers, jets, mixing layers, etc. The more problematic $\epsilon$ equation, which is used to determine the length scale in the $k$-$\epsilon$ model, is thus avoided.

In the present approach, the high turbulence Reynolds number ($Re_t = \sqrt{k}L/\nu \gg 1$) form of the $k$ equation is solved, together with a near-wall treatment, which depends on whether the flow is attached or detached. For attached flows, Gorski's[4] algebraic viscous sublayer treatment is used whereas, for detached flows, the algebraic backflow turbulence model of Goldberg and Chakravarthy[2] is invoked.

The $k$ and $L$ distributions are combined to form an eddy-viscosity ($\mu_t$) field that is added to the molecular viscosity in the diffusion terms of the Reynolds-averaged Navier-Stokes (RANS) equations. The high $Re_t$ $k$ equation, in two-dimensional Cartesian conservation form, reads as follows:

$$\frac{\partial}{\partial t}(\rho k) + \frac{\partial}{\partial x}(\rho u k) + \frac{\partial}{\partial y}(\rho v k) = \frac{1}{Re}\left\{\left[\frac{\partial}{\partial x}\left(\mu_k \frac{\partial k}{\partial x}\right) + \frac{\partial}{\partial y}\left(\mu_k \frac{\partial k}{\partial y}\right)\right] + P - D + i_{\mathrm{AXI}}\left(\frac{\mu_k}{y}\frac{\partial k}{\partial y} - \frac{\rho v k}{y} Re\right)\right\} \quad (1)$$

where the production term is given by

$$P = \mu_t\left\{\left(\frac{\partial u}{\partial y} + \frac{\partial v}{\partial x}\right)^2 + 2\left[\left(\frac{\partial u}{\partial x}\right)^2 + \left(\frac{\partial v}{\partial y}\right)^2\right]\right\}$$

the dissipation term is given by

$$D = \rho C_d \frac{k^{3/2}}{L} Re \qquad (C_d \approx 0.89)$$

the eddy viscosity is determined by

$$\mu_t = C_\mu \rho \sqrt{k} L Re \qquad (C_\mu \approx 0.09)$$

and the combined viscosity is

$$\mu_k = \mu + \mu_t/\sigma_k \qquad (\sigma_k \approx 1.0)$$

In Eq. (1), $i_{\mathrm{AXI}} = 1$ for axisymmetric flows and 0 for two-dimensional flows. The reference Reynolds number is $Re$, $[Re = U_{\mathrm{ref}} L_{\mathrm{ref}}/\nu_{\mathrm{ref}}]$, where the reference scales are an arbitrary self-consistent set used to nondimensionalize the equations of motion.

The length scale is composed of two parts (see Fig. 1): an inner branch and an outer branch. The outer branch consists of two linear sections given by

$$L_{\mathrm{out}} = C_L\left[(\delta - \Delta)\frac{y}{C_\mu \delta/\kappa} + \Delta\right], \qquad y < C_\mu \delta/\kappa$$

$$= C_L \delta, \qquad y \geq C_\mu \delta/\kappa$$

where $\delta$ is a measure of the local shear-layer thickness, determined as the distance from the wall (or wake core) to the location where the vorticity diminishes to below $10^{-4}$ times its local maximum value,‡ $\Delta$ is the distance from the core of

Received Oct. 26, 1988; revision received May 24, 1989. 

*Member Technical Staff. Member AIAA.
†Manager, CFD Department. Member AIAA.

‡Tolerance values of $10^{-5}$ and $10^{-6}$ produced no significant changes in the magnitude of $\delta$.

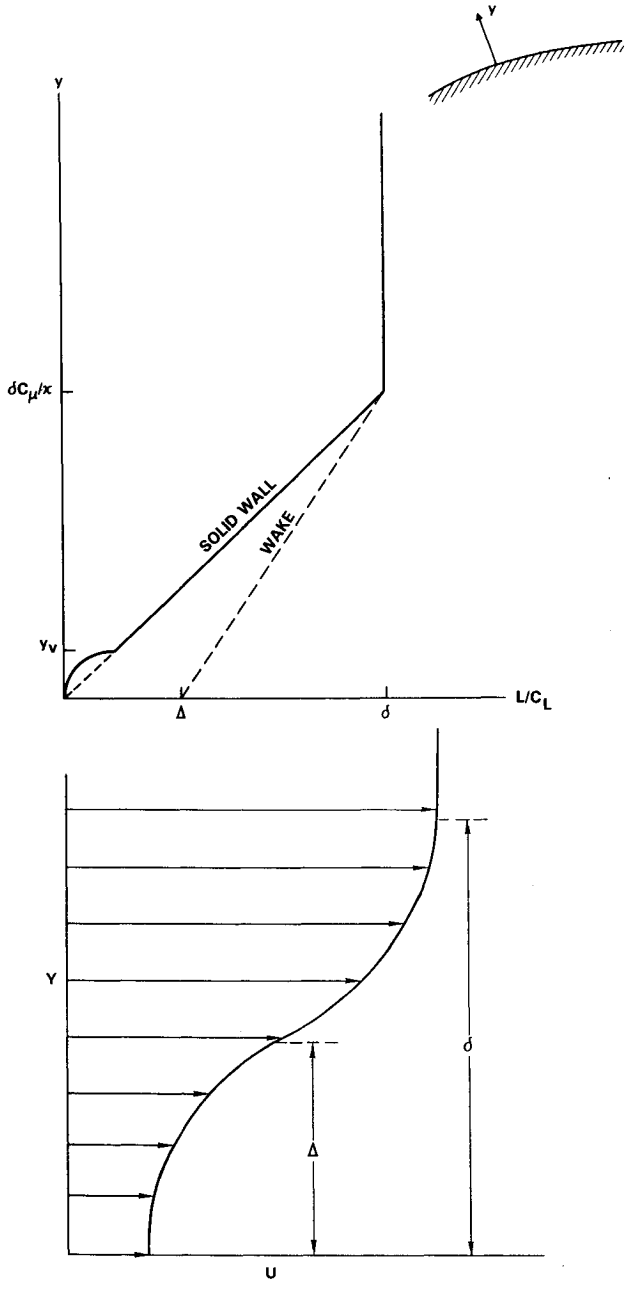


**Fig. 1 The *k-L* model length scale profile and nomenclature.**

the wake (if one exists) to the location of local maximum vorticity (see Fig. 1), and $\kappa \approx 0.4$ is the von Kármán constant. Note that the choice of $\Delta$ enables a smooth transition from wall-bounded flows to fully turbulent wakes. Thus, the outer scale grows linearly from zero (for solid surfaces) or $C_L\Delta$ (for wakes) to $C_L\delta$, its maximum value, which is reached when $y/\delta = C_\mu/\kappa \approx 0.2$. The value of $C_L$ depends on the local flow conditions through the interaction between the turbulence and the mean flow. Although a functional dependence of $C_L$ on the mean flow has not been established, a value of 0.27 was found satisfactory for a large number of problems across the Mach number range.

For solid surfaces, the inner length scale is determined by the behavior of the kinetic energy of turbulence and its dissipation within the viscous sublayer (see the following subsection, "Near-Wall Treatment"). In general, $L \sim k^{3/2}/\epsilon$ and after substituting for $k$ and $\epsilon$ their sublayer formulation, the result is

$$(L_{\text{in}})_{\text{wall}} = \alpha \frac{\rho_v \rho_w^{1/2}}{\rho^{3/2}} \frac{y^3}{y_v^2}, \qquad \alpha \approx 8.9$$

where subscripts $v$ and $w$ stand for sublayer edge and wall, respectively. Thus, for solid surfaces, the length scale grows as $y^3$ from zero at the wall until it reaches a magnitude corresponding to $L_{\text{out}}$. This occurs in the vicinity of the viscous sublayer edge, at which point $L$ is determined by the outer branch. For wall-bounded flows, the length scale is, therefore, given as (see Fig. 1)

$$L = \min\{L_{\text{in}}, L_{\text{out}}\}$$

**Near-Wall Treatment**

1. *Attached Flow*

Following Gorski,[4] $k$ and $\mu_t$ within the viscous sublayer are determined algebraically from the following formulas:

$$\rho_s k_s = \rho_v k_v \left(\frac{y_s}{y_v}\right)^2 \qquad 0 \le y_s \le y_v$$

$$\mu_{t_s} = \rho_s C_s \frac{1}{y_s^+} \frac{k_s^2}{\epsilon_s}$$

where the viscous sublayer edge $y_v$ is located at

$$y_v = 20\nu_w \frac{C_\mu^{1/4}}{u_\tau}, \qquad u_\tau = (\tau_w/\rho_w)^{1/2}$$

and the value of $k$ at the sublayer edge is

$$k_v = \frac{u_\tau^2}{\sqrt{C_\mu}} \frac{\rho_w}{\rho_v}$$

The value of the dissipation $\epsilon$ within the sublayer is given by

$$\epsilon_s = 2\nu_w \frac{k_v}{y_v^2}$$

Finally, the linear interpolator $C_s$ is given by

$$C_s = C_\mu + (C_{s_v} - C_\mu)\frac{y_s}{y_v}$$

where

$$C_{s_v} = 2\kappa\sqrt{(\rho_v/\rho_w)C_\mu}$$

2. *Detached Flow*

For detached flow, $k$ and $\mu_t$ within the backflow region are determined algebraically using the backflow turbulence model of Goldberg and Chakravarthy.[5] For details, see the Appendix.

**Initial and Boundary Conditions for Eq. (1)**

As initial conditions, a small nonzero value is prescribed for $k$ in the entire computational domain. Typically, $k/U_\infty^2 = 10^{-4}$ is used.

At a solid surface, $k$ is set to zero. This is done even though Eq. (1) does not apply in the near vicinity of walls. The justification is that $k$ is replaced in the near-wall region as described earlier. If the shear layer is in a wake region or if a slip wall boundary condition applies, the normal derivative of $k$ is set to zero: $(\partial k/\partial y)_w = 0$.

## Results

The hybrid *k-L*/backflow model has been incorporated into a finite-volume unified time/space marching zonal RANS code,[6,7] featuring an implicit upwind-biased scheme and total variation diminishing (TVD) discretization for high accuracy. Line Gauss Seidel relaxation was used for space marching, whereas the approximate factorization method was employed for time marching.

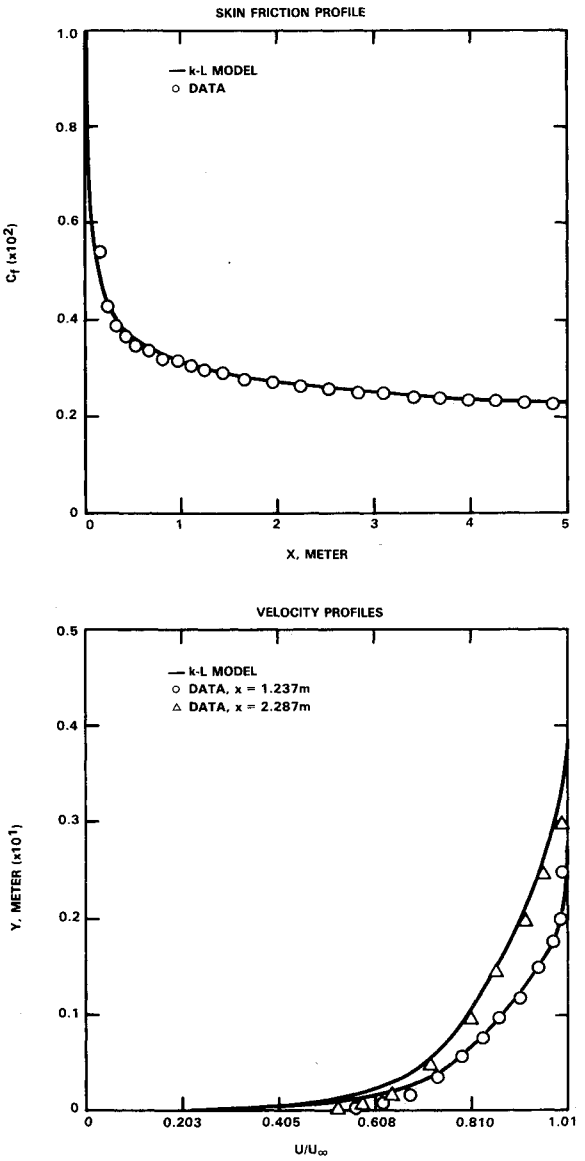


Fig. 2 Turbulent flow over a flat plate: comparison between predictions and data.

As a first validation case, turbulent flow over a flat plate was computed using a $100 \times 35$ grid and was compared with the experimental data of Wieghardt[8] at Mach 0.1. Figure 2 shows skin-friction and velocity-profile comparisons for two locations. The level of agreement is very encouraging.

Next, the axisymmetric bump flow experiment at $M_\infty = 0.875$ by Bachalo and Johnson[9] was computed using a $75 \times 36$ grid and was compared with data[9] as well as with calculations using the Johnson-King (J-K) turbulence model.[10] Figure 3 shows wall-pressure, skin-friction, and two velocity profiles in the detached flow region. In general, the current turbulence model produces results very similar to those obtained with the J-K model.

As a further validation case, a Mach 2.85 flow over a 24-deg ramp has been computed and compared with data by Settles et al.[11,12] and by Dolling and Murphy.[13] Figure 4 shows wall-pressure, skin-friction, and corner-velocity profiles resulting from a calculation done on a coarse $(60 \times 40)$ grid. The pressure prediction follows the data of Dolling and Murphy,

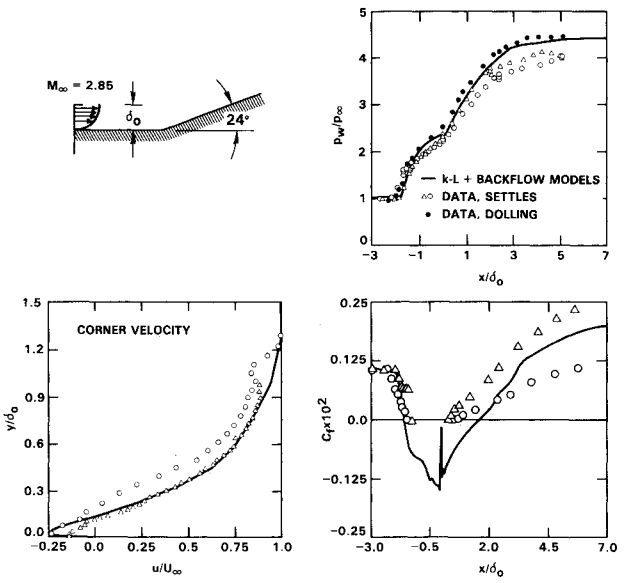


Fig. 4 Mach 3 24-deg compression corner flow problem: wall-pressure, skin-friction, and velocity-profile comparisons.

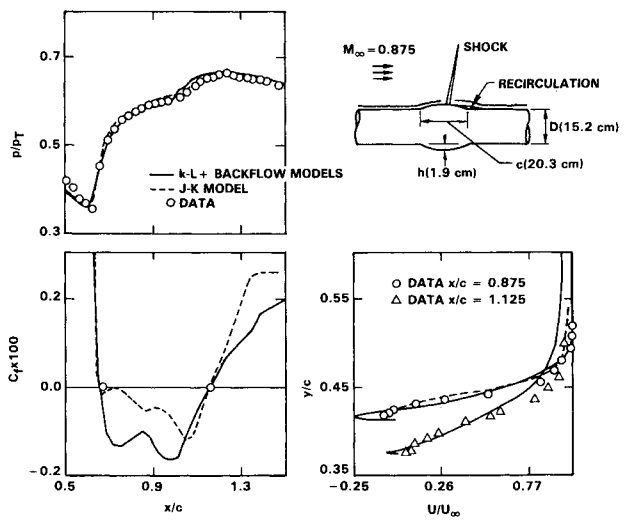


Fig. 3 Mach 0.9 axisymmetric bump flow problem: wall-pressure, skin-friction, and velocity-profiles comparisons.

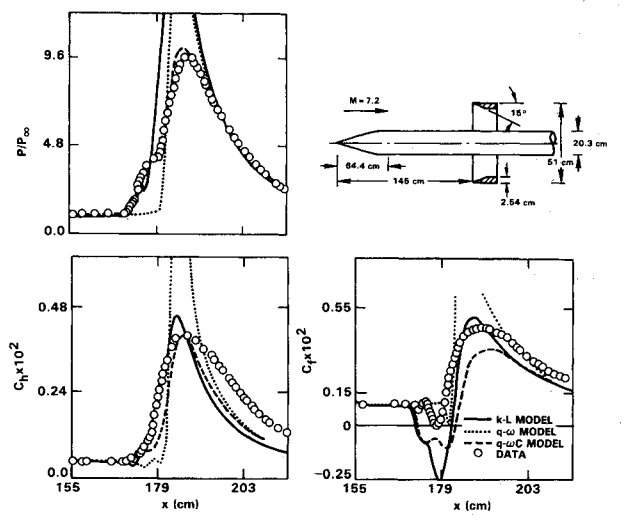


Fig. 5 Mach 7 ogive-cylinder shock/boundary-layer interaction flow problem: wall-pressure, heat-transfer, and skin-friction comparisons.

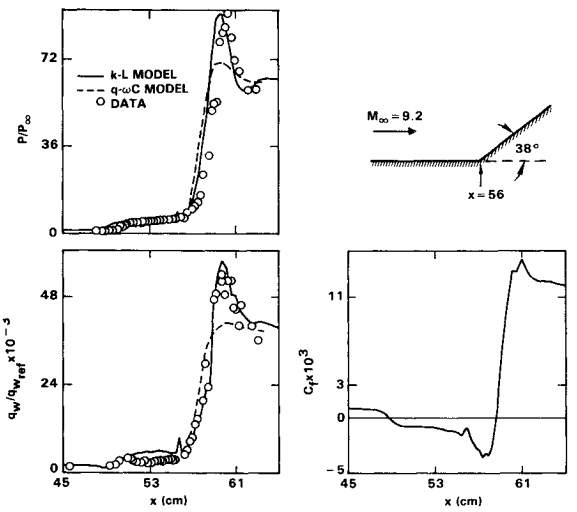


**Fig. 6 Mach 9 38-deg compression corner flow problem: wall-pressure and heat-transfer comparisons and skin-friction prediction.**

whereas the skin-friction and velocity predictions straddle the two data sets of Settles et al. except for a delayed reattachment.

The next two cases are in the hypersonic flow regime. Experimental data were obtained by Horstman et al.[14] for a Mach 7.2 flow over an axisymmetric ogive-cylinder configuration with a shock-generator ring. Figure 5 shows surface-pressure, heat-transfer, and skin-friction comparisons between the current model, experimental data for a 15-deg shock generator angle, and calculations by Vuong and Coakley[15] using the $q$-$\omega$ and $q$-$\omega c$ turbulence models (the latter being a $q$-$\omega$ model corrected for hypersonic effects). The computations were done on similar grids. In the present work, the shock generator was treated as an adiabatic surface over which a laminar boundary layer developed. At the trailing edge of the shock generator, located at $x = 154.48$ cm (measured from the nose of the ogive), an expansion took place. This expansion interacted with the shock reflecting from the cylinder surface. Both the $q$-$\omega c$ and the $k$-$L$ models predict the upstream influence rather well; the $k$-$L$ model, however, predicts a large post-reattachment pressure overshoot, as does the original $q$-$\omega$ model. The heat-transfer and skin-friction predictions are similar to those produced by the $q$-$\omega c$ model, but the branches corresponding to heat-transfer buildup are better predicted by the $k$-$L$ model.

The last comparison is for a Mach 9.2 flow over a 38-deg compression ramp, for which experimental data are available by Coleman and Stollery.[16] Figure 6 shows surface-pressure and heat-transfer comparisons between predictions (using a $100 \times 50$ grid) and data, as well as skin-friction prediction. Upstream influence is predicted very well, and pressure and heat-transfer levels are calculated correctly, both in the large backflow region and in the post-reattachment zone. A calculation using the $q$-$\omega c$ turbulence model[15] is also shown. The $k$-$L$ model predicts the post-reattachment behavior better, particularly the peaks in both pressure and heat transfer.

## Conclusions

A new hybrid $k$-$L$/backflow one-equation turbulence model has been introduced and demonstrated for several flow problems across the Mach number range, including detached flow regions. The special features of this model are the near-wall treatments for $k$, $L$, and $\mu_t$ under both attached and detached flow conditions, obviating the need to use wall functions whose validity, especially for detached flows, is highly questionable. The level of agreement between computations and experimental data suggests that this model is a promising one. Further results using it will be reported in future work.

## Appendix

The following algebraic distribution of eddy viscosity is prescribed throughout the backflow region (see Fig. A1 for definitions of the nomenclature):

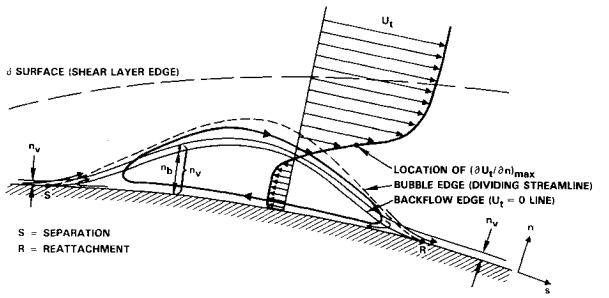


**Fig. A1 Schematic of detached flow bubble and nomenclature.**

$$\nu_t = u_s n_v \sqrt{\rho_w/\rho}\, \mathcal{G}^{1/2}(s,n)[A(n/n_b)+B]/(2\sqrt{2}\beta^2) \qquad 0 \le n \le n_b$$

wake term; near wall term; low Reynolds number term

where

$$\frac{n_v}{n_b} = 1 + 20\left(\frac{\nu_w}{u_s n_b}\right) C_\mu^{1/4}$$

$$\mathcal{G}(s,n) = \frac{\rho k}{\rho_b k_b} = [1 - e^{-\phi(n/n_b)^2}]/[1 - e^{-\phi}]$$

$$\beta = k_v/k_b = 1 + [(n_v/n_b)^2 - 1]\phi/(e^\phi - 1)$$

$$u_s = \sqrt{(-\overline{uv})_{\max}} = \sqrt{\nu_{t,m}(\partial U_t/\partial n)_{\max}}$$

$$\nu_{t,m} = \nu_t \,|_{\partial U_t/\partial n = \max}$$

with

$$A = -(C_\mu^*/2)^{9/5}, \qquad B = (C_\mu^*/2)^{3/5} - A, \qquad C_\mu = 0.09$$

$$C_\mu^* = 0.2, \qquad \phi = 0.5$$

The development and rationale for this functional form is given in Ref. 5.

For high Reynolds number flows, the preceding formula, for all practical purposes, can be reduced to

$$(\nu_t)_{\text{inner}} = C_1 u_s n_b \sqrt{\rho_w/\rho}[A(n/n_b)+B]\sqrt{\mathcal{G}(s,n)} \qquad 0 \le n \le n_b$$

$$(\nu_t)_{\text{outer}} = C_2 u_s n_b \sqrt{\rho_w/\rho}, \qquad n > n_b$$

where

$$C_1 \approx 0.353, \qquad C_2 \approx C_1(C_\mu^*/2)^{3/5}$$

## References

[1]Goldberg, U. C., and Chakravarthy, S. R., "Prediction of Separated Flows with a New Turbulence Model," *Proceedings of the 5th International Conference on Numerical Methods in Laminar and Turbulent Flow*, Pt. 1, edited by Taylor, Habashi, and Hafez, Pineridge

Press Limited, Swansea, UK, July 1987, pp. 560–571.

[2]Goldberg, U. C., and Chakravarthy, S. R., "Prediction of Separated Flows with a New Backflow Turbulence Model," *AIAA Journal,* Vol. 26, No. 4, 1988, pp. 405–408.

[3]Goldberg, U. C., "Separated Flow Predictions Using a New Turbulence Model," *Proceedings of the 6th Symposium on Turbulent Shear Flows,* Sept. 1987, pp. 15.5.1–15.5.6.

[4]Gorski, J. J., "A New Near-Wall Formulation for the $k$-$\epsilon$ Equations of Turbulence," AIAA Paper 86-0556, Jan. 1986.

[5]Goldberg, U. C., "Separated Flow Treatment with a New Turbulence Model," *AIAA Journal,* Vol. 24, No. 10, 1986, pp. 1711–1713.

[6]Chakravarthy, S. R., Szema, K.-Y., Goldberg, U. C., Gorski, J. J., and Osher, S., "Application of a New Class of High Accuracy TVD Schemes to the Navier-Stokes Equations," AIAA Paper 85-0165, Jan. 1985.

[7]Chakravarthy, S. R., "The Versatility and Reliability of Euler Solvers Based on High-Accuracy TVD Formulations," AIAA Paper 86-0243, Jan. 1986.

[8]Weighardt, K., "Flat Plate Flow," *Proceedings of the AFOSR-IFP-Stanford Conference on Computaion of Turbulent Boundary Layers,* Vol. 2, edited by D. E. Coles and E. A. Hirst, Stanford Univ., 1968, pp. 98–123.

[9]Bachalo, W. D., and Johnson, D. A., "An Investigation of Transonic Turbulent Boundary Layer Separation Generated on an Axisymmetric Flow Model," AIAA Paper 79-1479, 1979.

[10]Johnson, D. A. and King, L. S., "A Mathematically Simple Turbulence Closure Model for Attached and Separated Turbulent Boundary Layers," *AIAA Journal,* Vol. 23, No. 11, 1985, pp. 1684–1692.

[11]Settles, G. S., Vas, I. E., and Bogdonoff, S. M., "Details of a Shock-Separated Turbulent Boundary-Layer at a Compression Corner," *AIAA Journal,* Vol. 14, No. 12, 1976, pp. 1709–1715.

[12]Settles, G. S., Fitzpatrick, T. J., and Bogdonoff, S. M., "Detailed Study of Attached and Separated Compression Corner Flow Fields in High Reynolds Number Supersonic Flow," *AIAA Journal,* Vol. 17, No. 6, 1979, pp. 579–585.

[13]Dolling, D. S. and Murphy, M. T., "Unsteadiness of the Separation Shock Wave Structure in a Supersonic Compression Ramp Flowfield," *AIAA Journal,* Vol. 21, Dec. 1983, pp. 1628–1634.

[14]Horstman, C. C., Kussoy, M. I., Coakley, T. J., Rubesin, M. W., and Marvin, J. G., "Shock-Wave Induced Turbulent Boundary-Layer Separation at Hypersonic Speeds," AIAA Paper 75-4, Jan. 1975.

[15]Vuong, S. T., and Coakley, T. J., "Modeling of Turbulence for Hypersonic Flows with and without Separation," AIAA Paper 87-0172, 1987.

[16]Coleman, G. T., and Stollery, J. L., "Heat Transfer in Hypersonic Turbulent Separated Flow," Imperial College of Science and Technology, Department of Aeronautics, London, UK, Report 72-05, March 1972.